Recent improvements of a high-cycle accumulation model for sand

T. Wichtmann, A. Niemunis, Th. Triantafyllidis [1]

Summary

The paper addresses recent improvements of the authors' high-cycle accumulation (HCA) model, in particular with regard to the prediction of permanent deformations of offshore wind power plant foundations. The calibration of the HCA model for a typical North Sea fine sand is presented. The elastic stiffness E *of the model has been examined in drained and undrained cyclic triaxial tests. Based on data from approx. 350 drained cyclic triaxial tests performed on 22 quartz sands with different grain size distribution curves a simplified calibration procedure has been developed. Correlations of the HCA model parameters with mean grain size* d_{50}*, coefficient of uniformity* C_u *and minimum void ratio* $e_{\min}$ *are proposed for that purpose.*

1 Introduction

Numerous offshore wind parks will be installed in the North Sea and in the Baltic Sea during the next years. The foundations of offshore wind power plants (OWPPs) are subjected to a multiaxial high-cyclic loading due to wind and waves, which may cause an accumulation of permanent deformations. The serviceability of the OWPPs may get lost due to an excessive tilting of the tower. As discussed elsewhere [Wichtmann et al., 2008, 2010b], no established methods for a prediction of the long-term deformations exist so far. Furthermore, experience from conventional offshore foundations (e.g. oil rigs) or from existing much smaller OWPP foundations cannot be easily adapted.

The authors intend to apply their high-cycle accumulation (HCA) model [Niemunis et al., 2005] in order to predict the permanent deformations of OWPP foundations. Some recent improvements of the HCA model are addressed in the present paper, amongst others:

- The stiffness E of the HCA model has been inspected in several drained and undrained cyclic triaxial tests. Despite its importance for stress relaxation (e.g. decrease of horizontal stress acting on a pile foundation), E has been rarely studied up to now.
- A simplified calibration procedure based on granulometric properties and index quantities has been established based on approx. 350 drained cyclic triaxial tests performed on 22 clean quartz sands with different grain size distribution curves.

[1] Institute for Soil Mechanics and Rock Mechanics (IBF), Karlsruhe Institute of Technology (KIT)

Influence	Function	Parameter	Value
Strain amplitude	$f_{\text{ampl}} = \left(\varepsilon^{\text{ampl}}/10^{-4}\right)^{C_{\text{ampl}}}$	C_{ampl}	1.31
Void ratio	$f_e = \dfrac{(C_e - e)^2}{1+e} \dfrac{1+e_{\max}}{(C_e - e_{\max})^2}$	C_e	0.58
Average mean pressure	$f_p = \exp\left[-C_p \ (p^{\text{av}}/100 - 1)\right]$	C_p	0.22
Average stress ratio	$f_Y = \exp\left(C_Y \ \bar{Y}^{\text{av}}\right)$	C_Y	1.85
Cyclic preloading	$\dot{f}_N = \dot{f}_N^A + \dot{f}_N^B$	C_{N1}	$2.82 \cdot 10^{-4}$
	$\dot{f}_N^A = C_{N1} C_{N2} \exp\left[-g^A/(C_{N1} f_{\text{ampl}})\right]$	C_{N2}	0.37
	$\dot{f}_N^B = C_{N1} C_{N3}$	C_{N3}	$2.64 \cdot 10^{-5}$
Polarization changes	f_π, see [Niemunis et al., 2005]		

Table 1: HCA model functions and parameters for a fine sand ($e_{\min}$ = 0.677, $e_{\max}$ = 1.054)

2 High cycle accumulation model

The main constitutive equation of the HCA model reads

$$\dot{\boldsymbol{\sigma}} = \mathsf{E} : (\dot{\boldsymbol{\varepsilon}} - \dot{\boldsymbol{\varepsilon}}^{\text{acc}} - \dot{\boldsymbol{\varepsilon}}^{\text{pl}}) \tag{1}$$

with the Jaumann stress rate $\dot{\boldsymbol{\sigma}}$ of the effective Cauchy stress $\boldsymbol{\sigma}$, the strain rate $\dot{\boldsymbol{\varepsilon}}$, the prescribed strain accumulation rate $\dot{\boldsymbol{\varepsilon}}^{\text{acc}}$, the plastic strain rate $\dot{\boldsymbol{\varepsilon}}^{\text{pl}}$ (for stress paths touching the yield surface only) and the pressure-dependent elastic stiffness E. In the high-cyclic context "rate" means the derivative with respect to the number of cycles N. The accumulation rate is calculated as the product of the scalar *intensity* of accumulation $\dot{\varepsilon}^{\text{acc}}$ and the *direction* of accumulation $\mathbf{m}$ (unit tensor):

$$\dot{\boldsymbol{\varepsilon}}^{\text{acc}} \ = \ \dot{\varepsilon}^{\text{acc}} \, \mathbf{m} \ = \ f_{\text{ampl}} \ \dot{f}_N \ f_e \ f_p \ f_Y \ f_\pi \ \mathbf{m} \tag{2}$$

The flow rule of the modified Cam clay (MCC) model has been experimentally found to approximate $\mathbf{m}$ well. A multiplicative approach is used for $\dot{\varepsilon}^{\text{acc}}$. Each function considers separately the influence of a specific parameter (Table 1). The spatial field of the strain amplitude can be obtained from a calculation of a few cycles using a conventional constitutive model. The authors use hypoplasticity with intergranular strain [von Wolffersdorff, 1996, Niemunis and Herle, 1997] for that purpose.

For calculations with the HCA model the following parameters have to be determined or estimated:

- Seven parameters C_{ampl}, C_e, C_p, C_Y, C_{N1}, C_{N2} and C_{N3} for the intensity of accumulation $\dot{\varepsilon}^{\text{acc}}$ (see Table 1). If the effect of polarization changes (function f_π) shall be considered, two more parameters are necessary [Niemunis et al., 2005].
- One parameter (critical friction angle φ_c) for the cyclic flow rule $\mathbf{m}$.

- Two parameters (bulk modulus K and Poisson's ratio ν) for the isotropic elastic stiffness E.
- The parameters for the conventional constitutive model used for the determination of the spatial field of the strain amplitude.

3 Calibration procedure

The calibration procedure is demonstrated by means of test data for a uniform fine sand ($d_{50} = 0.14$ mm, $C_u = d_{60}/d_{10} = 1.5$). This sand is also currently in use in small-scale model tests on OWPP foundations performed at our institute [Wienbroer et al., 2010, Solf et al., 2010].

The critical friction angle $\varphi_c = 33.1°$ necessary for the cyclic flow rule $\mathbf{m}$ has been determined from the inclination of a pluviated cone of dry sand.

The parameters C_{ampl}, C_e, C_p, C_Y, C_{N1}, C_{N2} and C_{N3} have been determined from stress-controlled drained cyclic triaxial tests following the procedure described by [Wichtmann et al., 2010a]. 10^5 load cycles were applied at a frequency of 0.2 Hz. 16 tests with four different stress amplitudes q^{ampl}, seven different initial relative densities $I_{D0} = (e_{\max} - e_0)/(e_{\max} - e_{\min})$, four different average mean pressures p^{av} and four different average stress ratios $\eta^{\text{av}} = q^{\text{av}}/p^{\text{av}}$ were performed. Figure 1 shows a typical plot of the vertical strain $\varepsilon_1(t)$ measured during the first 24 cycles and during five cycles recorded at $N = 50, 100, 200, \ldots, 10^5$.

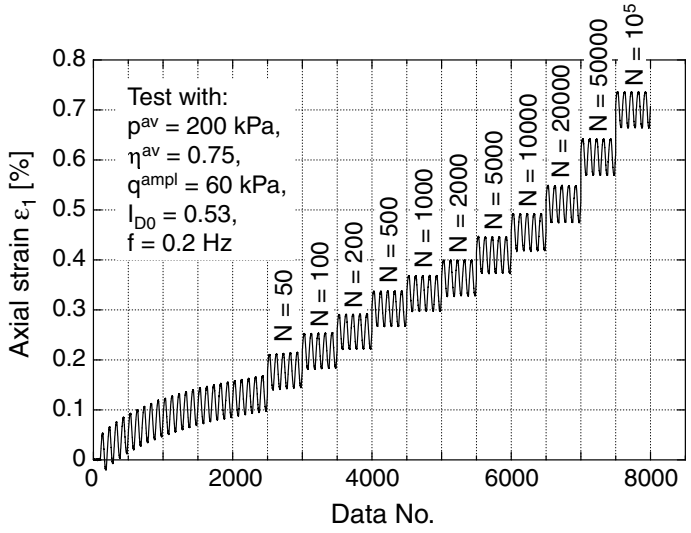

Figure 1: *Vertical strain $\varepsilon_1(t)$ measured during the initial phase of a drained cyclic triaxial test and after different numbers of cycles.*

The left column of diagrams in Figure 2 shows the increase of the residual strain ε^{acc} with increasing number of cycles N measured in the four test series. Evidently, the rate of

strain accumulation increases with increasing amplitude (Figure 2a), decreasing density (Figure 2c) and increasing average stress ratio (Figure 2g). Similar residual strains are obtained for different average mean pressures if the tests are performed with the same amplitude-pressure ratio $\zeta = q^{\mathrm{ampl}}/p^{\mathrm{av}}$ (Figure 2e).

The HCA model parameter C_{ampl} was determined from a curve-fitting of the function f_{ampl} (Table 1) to the data shown in Figure 2b. In that figure the residual strain $\varepsilon^{\mathrm{acc}}$ after different numbers of cycles is plotted versus a mean value of the strain amplitude, calculated as $\bar{\varepsilon}^{\mathrm{ampl}} = 1/N \int \varepsilon^{\mathrm{ampl}}(N)\mathrm{d}N$. This averaging is necessary since the tests have been performed stress-controlled and thus the strain amplitude decreases slightly with N (especially during the first 100 cycles). On the ordinate the residual strain has been divided by the void ratio function $\bar{f}_e$ of the HCA model in order to purify the data from the influence of slightly different initial densities and different compaction rates. $\bar{f}_e$ has been calculated with a mean value of void ratio $\bar{e} = 1/N \int e(N)\mathrm{d}N$. The parameter C_{ampl} given in Table 1 is the average of the values determined for different numbers of cycles.

A curve-fitting of the function f_e to the data in Figure 2d delivered the parameter C_e given in Table 1. In Figure 2d the residual strain has been divided by the amplitude function f_{ampl} in order to purify the data from the influence of slightly different strain amplitudes. The data are plotted versus a mean value of void ratio. Since f_{ampl} is necessary to purify the data in Figure 2d and f_e is used on the ordinate in Figure 2b, the determination of C_{ampl} and C_e has to be done by iteration.

The parameters C_p and C_Y (Table 1) were determined from a curve-fitting of the functions f_p and f_Y to the data in Figures 2f and 2h. In those diagrams the residual strain has been divided by the amplitude and void ratio functions and plotted versus p^{av} or $\bar{Y}^{\mathrm{av}}$, respectively, where $\bar{Y}^{\mathrm{av}}$ is a normalized stress ratio which is zero for isotropic stresses and 1 on the critical state line.

The curves $\varepsilon^{\mathrm{acc}}(N)$ from Figure 2 have been divided by the functions $\bar{f}_{\mathrm{ampl}}$, $\bar{f}_e$, f_p and f_Y of the HCA model (Figure 3) in order to determine the parameters C_{N1}, C_{N2} and C_{N3}. A curve-fitting of the function $f_N = C_{N1} \cdot [\ln(1 + C_{N2}\ N) + C_{N3}\ N]$ to the data in Figure 3 (solid curve) delivered the C_{Ni}-values specified in Table 1.

The calibration of the parameters for the elastic stiffness E is discussed in detail in Section 4.

Drained monotonic triaxial tests on dense samples and oedometric compression tests on loose and dense samples were performed in order to determine the hypoplastic parameters given in [Wichtmann et al., 2010b]. The procedure recommended by [Herle, 1997] was applied. The parameters of intergranular strain were determined from the strain amplitudes measured in the drained cyclic triaxial tests [Wichtmann et al., 2010b].

4 Stiffness E

The bulk modulus $K = \dot{u}/\dot{\varepsilon}_v^{\mathrm{acc}}$ can be obtained as the ratio of the rate of pore water pressure accumulation $\dot{u}$ in a stress-controlled undrained cyclic test and the rate of volumetric

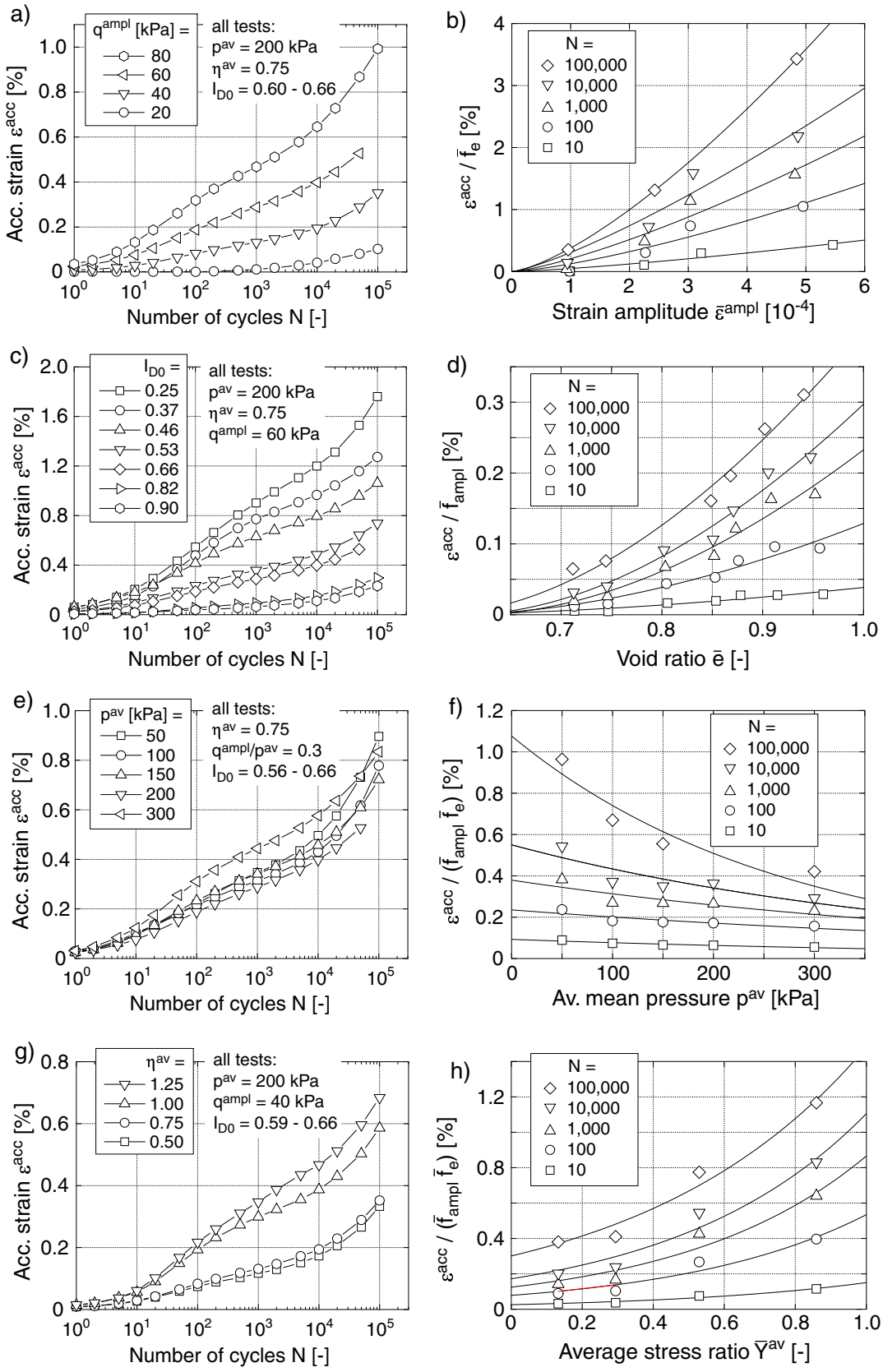

Figure 2: *Results of drained cyclic tests with different a,b) amplitudes, c,d) initial relative densities I_{D0}, e,f) average mean pressures p^{av} and g,h) average stress ratios η^{av}.*

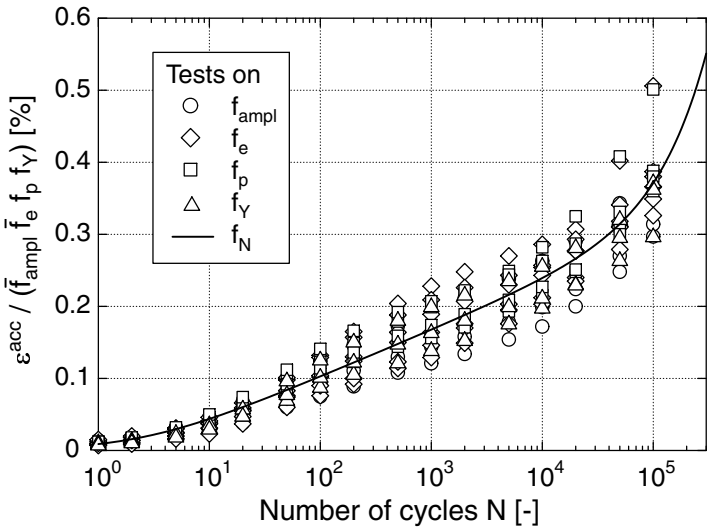

Figure 3: *Determination of parameters C_{Ni} from a curve-fitting of the function f_N to the curves $\varepsilon^{acc}(N)/(\bar{f}_{ampl}\bar{f}_e f_p f_Y)$.*

strain accumulation $\dot{\varepsilon}_v^{\mathrm{acc}}$ measured in a drained test. Both samples should have similar initial densities and the tests should be performed with identical consolidation stresses and cyclic loads.

Eight such test pairs have been performed on the fine sand so far. All specimens were prepared medium dense and consolidated isotropically. Different initial effective mean pressures in the range 50 kPa $\leq p_0 \leq$ 300 kPa and different amplitude-pressure ratios in the range $0.2 \leq \zeta = q^{\mathrm{ampl}}/p_0 \leq 0.3$ were tested (not all combinations have been tested so far). A typical undrained test result is shown in Figure 4 (development of pore water pressure with time) and Figure 5 (effective stress path). The accumulation of volumetric strain with increasing number of cycles in the drained tests is shown exemplary in Figure 6. Based on the test results the pressure-dependent bulk modulus (Figure 7) can be described by

$$K \;=\; A\,(p_{\mathrm{atm}})^{1-n}\,p^n \tag{3}$$

with $p^{\mathrm{atm}} = 100$ kPa and with constants $A = 467$ and $n = 0.46$. The same relationship has been found valid already for a medium coarse sand [**?**]. While the undrained test data for the medium coarse sand had to be purified from membrane penetration effects, such effects are negligible for the fine sand tested in the present study. For both sands, no significant influence of the amplitude on K could be detected.

The influence of soil density and stress anisotropy on K is presently being investigated. A first result of a stress-controlled undrained cyclic triaxial test with anisotropic consolidation stresses is shown in Figure 8. While the stress relaxation stops when the *maximum* stress during a cycle reaches the critical state line (Figure 8, CSL determined from undrained monotonic tests), the accumulation of axial strain continues. This experimental observation is not captured by the HCA model yet since the flow rule **m** predicts a decrease of p until the *average* stress reaches the CSL line.

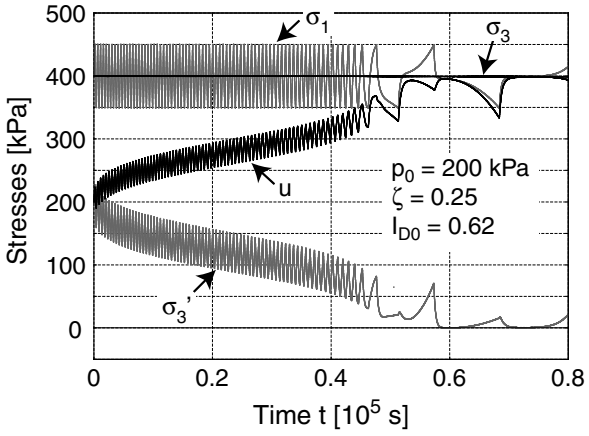

Figure 4: *Increase of pore water pressure and decrease of effective stress in a stress-controlled undrained cyclic triaxial test.*

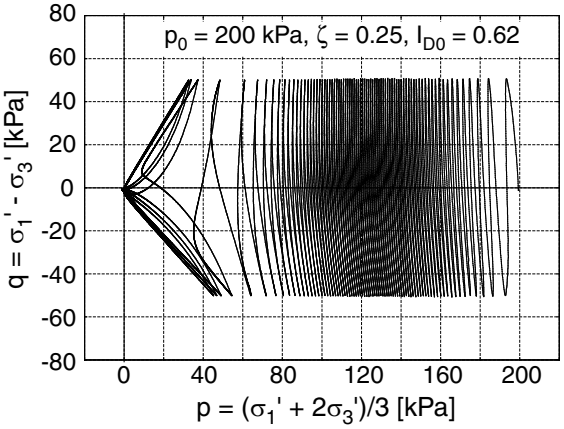

Figure 5: *Effective stress path in the p-q-plane in a stress-controlled undrained cyclic triaxial test.*

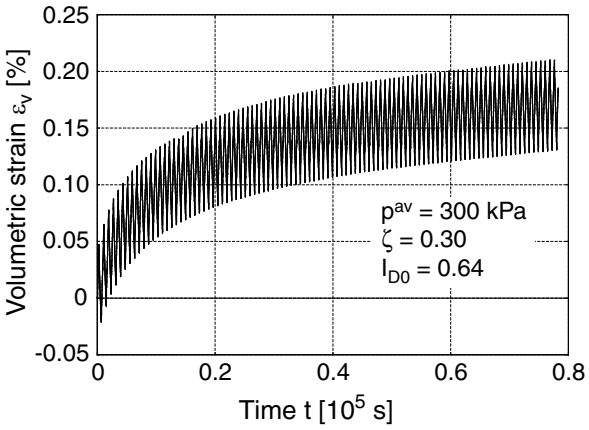

Figure 6: *Accumulation of volumetric strain in a stress-controlled drained cyclic triaxial test.*

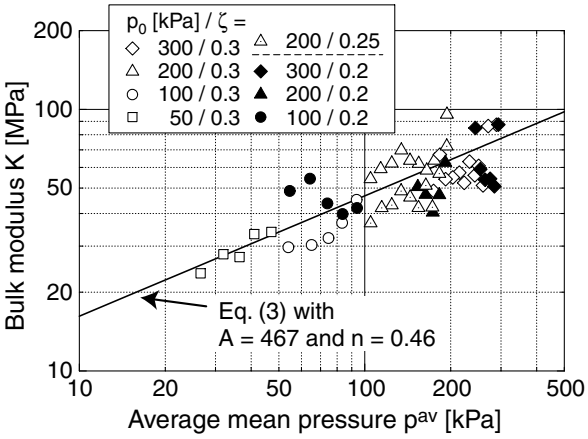

Figure 7: *Pressure-dependent bulk modulus $K = \dot{u}/\dot{\varepsilon}_v^{acc}$ derived from eight pairs of drained and undrained cyclic tests performed on fine sand.*

Poisson's ratio ν can be obtained from the shape of the average effective stress path in an undrained test with anisotropic consolidation stresses and strain cycles. A typical test result is shown in Figure 9. Several such tests showed no influence of the strain amplitude and the initial density on the shape of the average effective stress path (Figure 10). The first *irregular* cycle was applied drained in all tests so that the stress relaxation due to the subsequent *regular* cycles started from the same initial effective stress (the HCA model describes only the regular cycles). However, a test in which the first cycle was applied undrained showed the same average effective stress path (Figure 10). In order to investigate if the lubricated end plates (one layer of grease and membrane was used at each end) influence the relaxation of axial stress, a single test has been performed replacing the lubrication by a teflon foil. The results of this test did not differ from the tests with end lubrication (Figure 10).

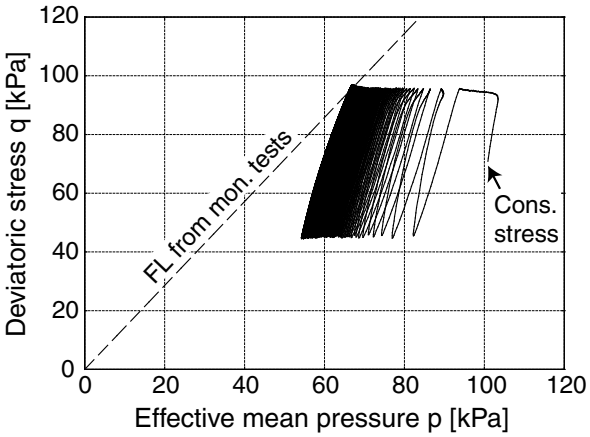

Figure 8: *Effective stress path in the p-q-plane in an undrained test with anisotropic consolidation stresses.*

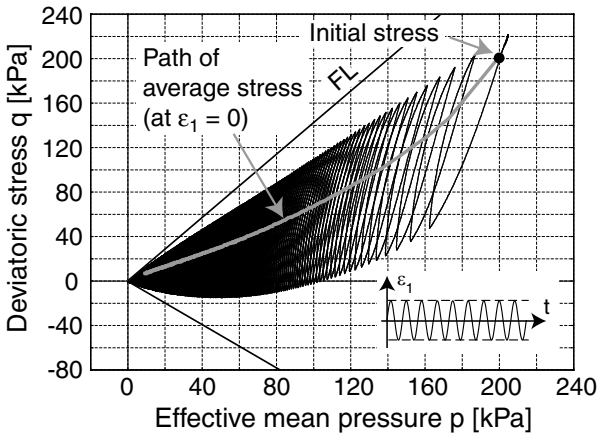

Figure 9: *Effective stress path in the p-q-plane in an undrained test with strain cycles.*

Average effective stress paths for different initial stress ratios $\eta_0 = q_0/p_0$ are presented in Figure 11. The optimum ν-values for a reproduction of these paths by the HCA model are given close to the initial stress of the tests. A Poisson's ratio of $\nu \approx 0.32$ was found appropriate for low to intermediate initial stress ratios $-0.75 \leq \eta_0 \leq 0.75$. The solid curves in Figure 11 were generated using $\nu \approx 0.32$. For initial stress ratios $\eta_0 > 0.75$ higher values of Poisson's ratio are necessary. Therefore, an isotropic elastic stiffness E may not suffice for large stress ratios.

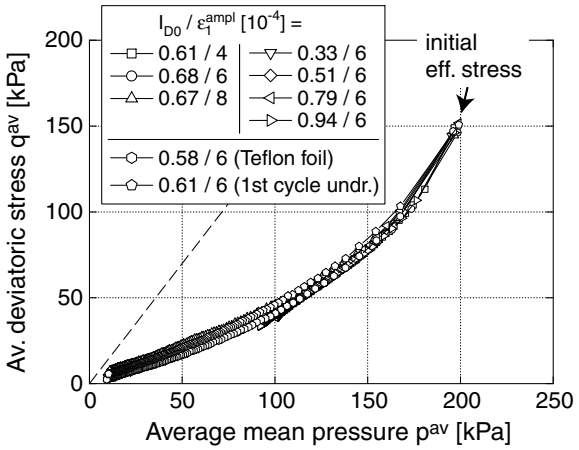

Figure 10: *Average effective stress paths in undrained tests with strain cycles and different amplitudes and initial densities.*

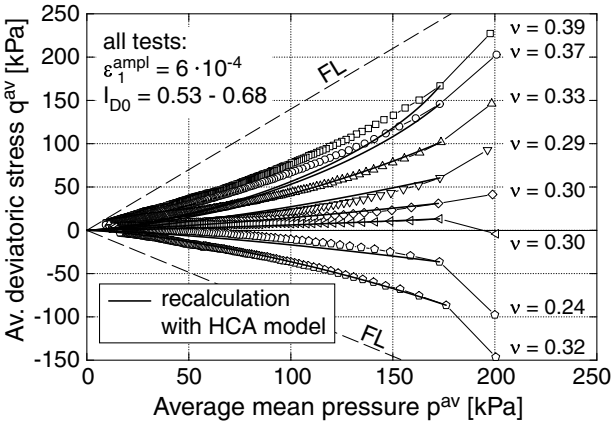

Figure 11: *Average effective stress paths in undrained triaxial tests with strain cycles commenced at different initial stress ratios $\eta_0 = q_0/p_0$.*

5 Simplified calibration using granulometric and index properties

The determination of the HCA model parameters C_{ampl}, C_e, C_p, C_Y, C_{N1}, C_{N2} and C_{N3} is quite laborious (Section 3). Regarding the large number of OWPPs in a wind park and the layered soil, an experimental determination of the parameters for each OWPP foundation and each soil type would be tedious. Therefore, a simplified calibration procedure has been already proposed by [Wichtmann et al., 2009] based on cyclic triaxial tests on eight quartz sands with different grain size distribution curves. Correlations of the HCA model constants with index properties (mean grain size d_{50}, coefficient of uniformity C_u, minimum void ratio $e_{\min}$) have been developed for that purpose. However, some of the correlations showed a significant amount of scatter.

Therefore, 14 more grain size distribution curves (Figure 12) with linear shape (in the semi-logarithmic scale) and with different mean grain sizes and coefficients of uniformity were tested in order to improve the correlations and to adapt them to a wider range of d_{50}- and C_u-values. The grain size distribution curves were mixed from a natural quartz sand with subangular grain shape. The sands and gravels L1 to L7 (Figure 12a) have mean grain sizes in the range 0.1 mm $\leq d_{50} \leq$ 3.5 mm and the same coefficient of uniformity $C_u = 1.5$. The materials L4 and L10 to L16 (Figure 12b) have the same mean grain size $d_{50} = 0.6$ mm while C_u varies between 1.5 and 8. Similar test series as shown in Figure 2 were performed on each sand.

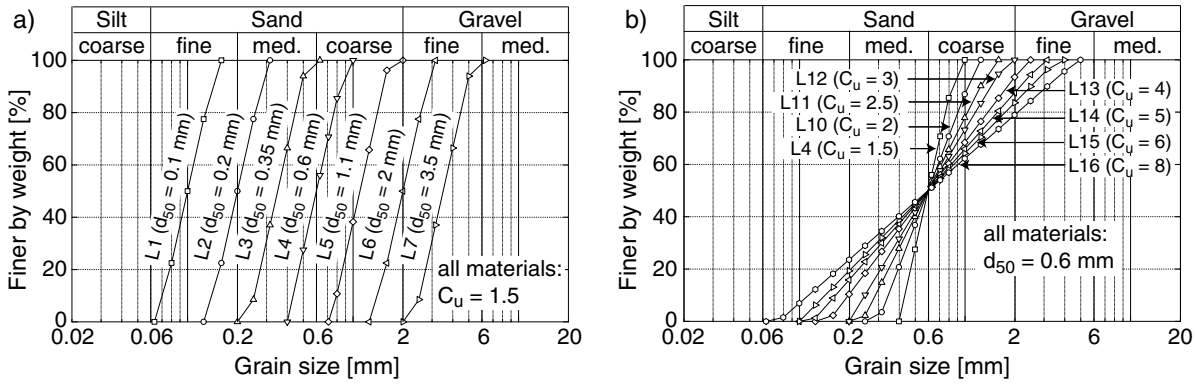

Figure 12: *Tested grain size distribution curves.*

The dependence of the intensity of accumulation $\dot{\varepsilon}^{\text{acc}}$ on the grain size distribution curve is inspected in Figure 13, where the residual strain after 10,000 cycles is plotted versus d_{50} or C_u, respectively. In accordance with [Wichtmann et al., 2009] the intensity of accumulation increases with decreasing mean grain size and with increasing coefficient of uniformity.

As an alternative to the "by hand" calibration outlined in Section 3, the HCA model parameters were also determined by means of a C++ program. It finds those parameters for which the sum of the squares of the differences between the experimentally obtained ε^{acc}-data and the data predicted by the HCA model takes its minimum. The method

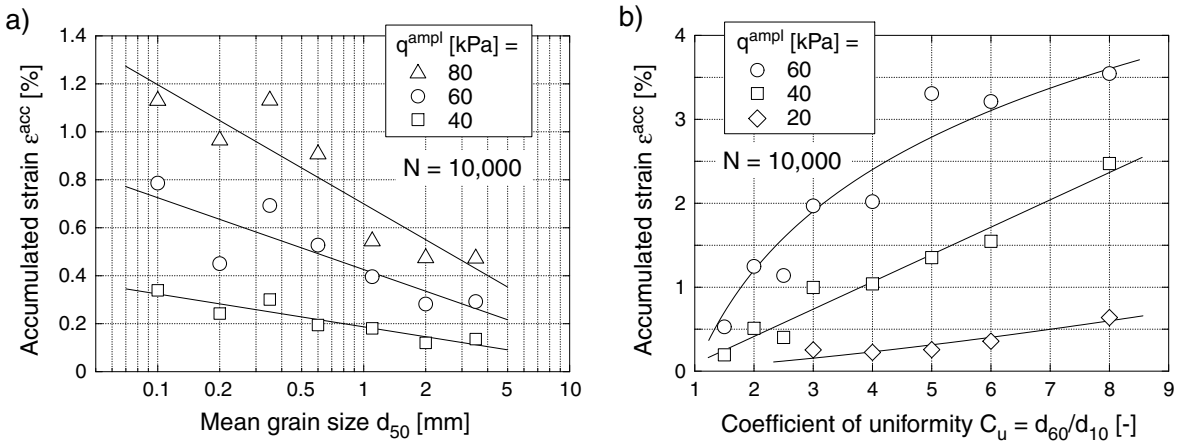

Figure 13: *Accumulated strain ε^{acc} as a function of a) mean grain size d_{50} and b) coefficient of uniformity C_u.*

may be seen as some kind of "fine tuning" of the parameters. The parameters obtained with the C++ program differ from those calibrated "by hand" due to simplifications of the "by hand" method (for example mean values $\bar{\varepsilon}^{\text{ampl}}$ and $\bar{e}$ are used in the diagrams, parameters determined for different N-values are averaged). The parameters C_{ampl}, C_e, C_p and C_Y were also estimated from the rate data (as described in [Wichtmann et al., 2010a]). The parameters C_{N1}, C_{N2} and C_{N3} were determined both, from the data of all tests and (simplified) from the three tests with different amplitudes only.

In Figure 14 the HCA model parameters are plotted versus mean grain size d_{50}, coefficient of uniformity C_u or minimum void ratio $e_{\min}$, respectively. The data from the tests described by [Wichtmann et al., 2009] were re-analyzed with $C_{\text{ampl}} \neq 2.0$ and are included in Figure 14. The correlations defined by Equations (4) to (10) are given in Figure 14 as solid lines and may be used for a simplified estimation of a set of parameters.

$$C_{\text{ampl}} = 1.70 \tag{4}$$

$$C_e = 0.95 \cdot e_{\min} \tag{5}$$

$$C_p = 0.41 \cdot [1 - 0.34\ (d_{50} - 0.6)] \tag{6}$$

$$C_Y = 2.60 \cdot [1 + 0.12\ \ln(d_{50}/0.6)] \tag{7}$$

$$C_{N1} = 4.5 \cdot 10^{-4} \cdot [1 - 0.306\ \ln(d_{50}/0.6)] \cdot [1 + 3.15\ (C_u - 1.5)] \tag{8}$$

$$C_{N2} = 0.31 \cdot \exp[0.39\ (d_{50} - 0.6)] \cdot \exp[12.3(\exp(-0.77 C_u) - 0.315)] \tag{9}$$

$$C_{N3} = 3.0 \cdot 10^{-5} \cdot \exp[-0.84\ (d_{50} - 0.6)] \cdot [1 + 7.85\ (C_u - 1.5)]^{0.34} \tag{10}$$

The parameter C_{ampl} does not correlate with d_{50} or C_u (Figure 14a,b). For C_e both, a correlation with d_{50} and C_u (Figure 14c,d) and with minimum void ratio $e_{\min}$ (Figure 14e) could be established. The values of C_p and C_Y plotted in Figure 14f-i were obtained calculating C_{ampl} and C_e from Equations (4) and (5). Similarly, the data for C_{N1}, C_{N2} and C_{N3} in Figure 14j-o have been analyzed with C_{ampl}, C_e, C_p and C_Y calculated from Equations (4) to (7). The poor correlation between C_{N3} and d_{50} can possibly be improved by means of data from tests with larger numbers of cycles ($N > 10^5$).

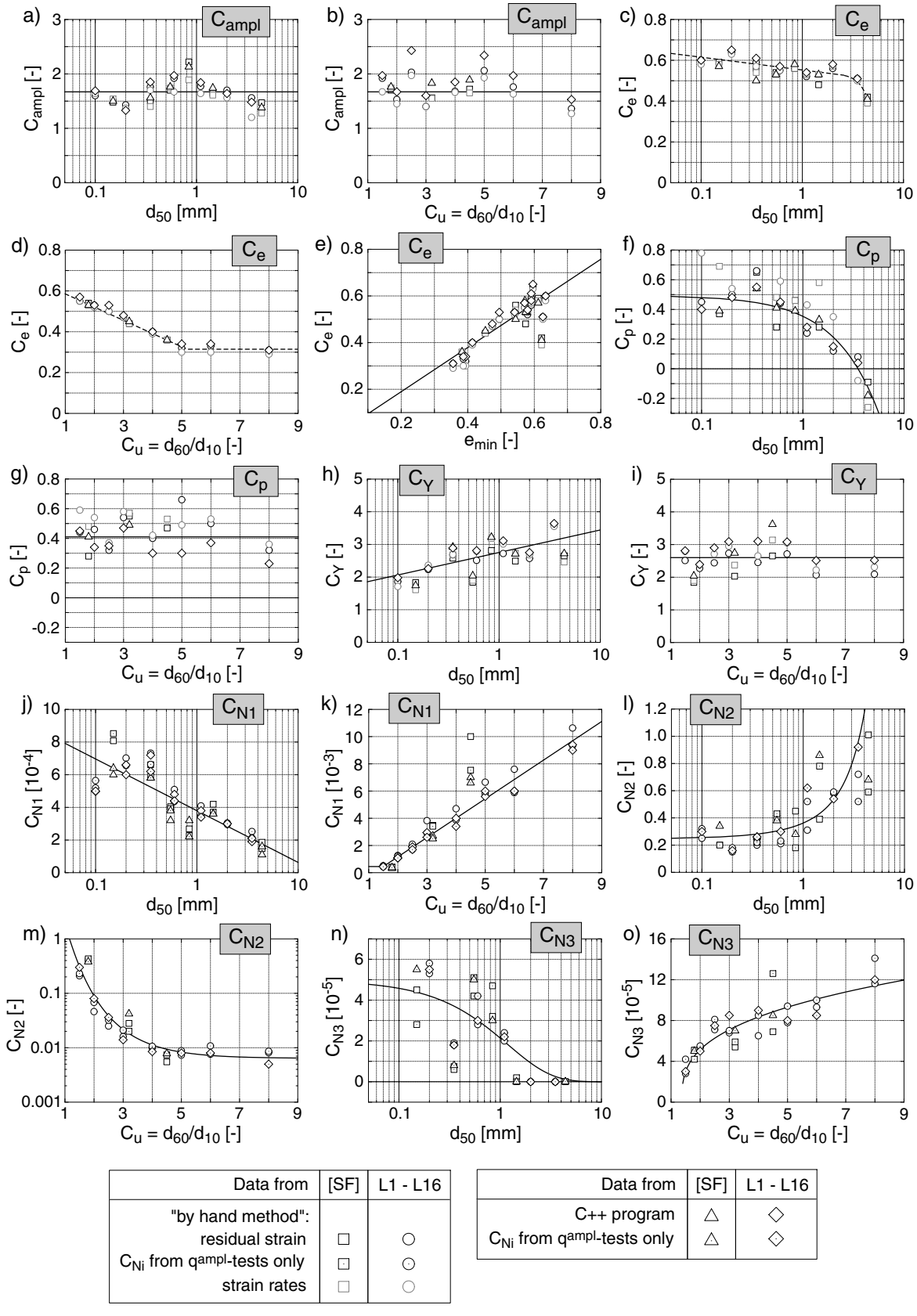

Data from	[SF]	L1 - L16
"by hand method":		
residual strain	□	○
C_{Ni} from q^{ampl}-tests only	□	○
strain rates	□	○

Data from	[SF]	L1 - L16
C++ program	△	◇
C_{Ni} from q^{ampl}-tests only	△	◇

Figure 14: *Correlations of the HCA model parameters with d_{50}, C_u or $e_{\min}$, respectively (SF = [Wichtmann et al., 2009]).*

6 Summary, conclusions and outlook

The elastic stiffness E of the high-cycle accumulation model has been examined for a fine sand. The pressure-dependent bulk modulus K has been derived from eight pairs of drained and undrained cyclic tests. It can be approximated by Equation (3) with the constants $A = 467$ and $n = 0.46$. At present, the influence of density and stress anisotropy on K is studied. Poisson's ratio ν has been determined from undrained tests with anisotropic consolidation stresses and strain cycles. ν has been found independent of amplitude and density. For low to intermediate stress ratios, $\nu = 0.32$ is appropriate.

Based on data from approx. 350 drained cyclic triaxial tests performed on 22 quartz sands with different grain size distribution curves a simplified procedure for the determination of the HCA model parameters C_{ampl}, C_e, C_p, C_Y, C_{N1}, C_{N2} and C_{N3} has been developed. Correlations of the HCA model parameters with mean grain size d_{50}, coefficient of uniformity C_u or minimum void ratio $e_{\min}$, respectively, have been formulated. In future the simplified calibration procedure will be extended to granular materials containing fines.

Since the OWPP foundations are subjected to a very large number of load cycles, long-term tests with $N \approx 10^8$ cycles are planned in order to evaluate the function f_N of the HCA model for large N-values. The effect of changes of the polarization of the cycles (factor f_π of the HCA model) will be studied in cyclic triaxial tests with a simultaneous oscillation of the axial and lateral stresses. In the case of OWPPs such changes are caused by the variation of the direction of wind and wave loading.

7 Acknowledgements

This work has been done in the framework of the project "Geotechnical robustness and self-healing of foundations of offshore wind power plants" funded by the German Federal Ministry for the Environment, Nature Conservation and Nuclear Savety (BMU) (grant No. 0327618). The authors are grateful to BMU for the financial support. The cyclic triaxial tests were performed by H. Borowski which is gratefully acknowledged.

Literature

I. Herle. Hypoplastizität und Granulometrie einfacher Korngerüste. Promotion, Institut für Bodenmechanik und Felsmechanik der Universität Fridericiana in Karlsruhe, Heft Nr. 142, 1997.

A. Niemunis and I. Herle. Hypoplastic model for cohesionless soils with elastic strain range. *Mechanics of Cohesive-Frictional Materials*, 2:279–299, 1997.

A. Niemunis, T. Wichtmann, and T. Triantafyllidis. A high-cycle accumulation model for sand. *Computers and Geotechnics*, 32(4):245–263, 2005.

O. Solf, P. Kudella, and Th. Triantafyllidis. Investigation of the self-healing effect of monopile foundations. In *International Conference on Physical Modelling in Geotechnics ICPMG 2010, Zurich*, 2010.

P.-A. von Wolffersdorff. A hypoplastic relation for granular materials with a predefined limit state surface. *Mechanics of Cohesive-Frictional Materials*, 1:251–271, 1996.

T. Wichtmann, A. Niemunis, and Th. Triantafyllidis. Prediction of long-term deformations for monopile foundations of offshore wind power plants. In *11th Baltic Sea Geotechnical Conference: "Geotechnics in Maritime Engineering", Gdańsk, Poland, 15-18 September 2008*, pages 785–792, 2008.

T. Wichtmann, A. Niemunis, and T. Triantafyllidis. Validation and calibration of a high-cycle accumulation model based on cyclic triaxial tests on eight sands. *Soils and Foundations*, 49 (5):711–728, 2009.

T. Wichtmann, A. Niemunis, and T. Triantafyllidis. On the determination of a set of material constants for a high-cycle accumulation model for non-cohesive soils. *Int. J. Numer. Anal. Meth. Geomech.*, 34(4):409–440, 2010a.

T. Wichtmann, A. Niemunis, and Th. Triantafyllidis. Towards the fe prediction of permanent deformations of offshore wind power plant foundations using a high-cycle accumulation model. In *International Symposium: Frontiers in Offshore Geotechnics, Perth, Australia*, 2010b.

H. Wienbroer, H. Zachert, G. Huber, P. Kudella, and Triantafyllidis Th. Experimental investigation of the self-healing effect of foundations for offshore wind turbine structures. In *2nd International Symposium on Frontiers in Offshore Geotechnics, Perth, Western Australia*, 2010.